Journal of Pharmaceutical and Biomedical Analysis 52 (2010) 391–397

Contents lists available at ScienceDirect

Journal of Pharmaceutical and Biomedical Analysis

journal homepage: www.elsevier.com/locate/jpba

Metabolism of sanguinarine in human and in rat: Characterization of oxidative metabolites produced by human CYP1A1 and CYP1A2 and rat liver microsomes using liquid chromatography–tandem mass spectrometry

Alain Deroussent[a,*], Micheline Ré[a], Henri Hoellinger[b], Thierry Cresteil[b]

[a] Institut de cancérologie Gustave Roussy, Research Department IFR54, Mass Spectrometry Facility, 39 rue Camille Desmoulins, 94805 Villejuif Cedex, France
[b] Institut de Chimie des Substances Naturelles, CNRS - UPR2301, 91190 Gif sur Yvette, France

ARTICLE INFO

Article history:
Received 2 July 2009
Received in revised form 5 September 2009
Accepted 10 September 2009
Available online 16 September 2009

Keywords:
Sanguinarine
Metabolism
Rat liver microsome
Human CYP1A
LC–MS/MS

ABSTRACT

The quaternary benzo[*c*]phenanthridine alkaloid, sanguinarine (SA), has been detected in the mustard oil contaminated with *Argemone mexicana*, which produced severe human intoxications during epidemic dropsy in India. Today, SA metabolism in human and in rat has not yet been fully elucidated. The goal of this study is to investigate the oxidative metabolites of SA formed during incubations with rat liver microsomes (RLM) and recombinant human cytochrome P450 (CYP) and to tentatively identify the CYP isoforms involved in SA detoxification. Metabolites were analyzed by liquid chromatography combined with electrospray ionization-tandem mass spectrometry. Up to six metabolites were formed by RLM and their modified structure has been proposed using their mass spectra and mass shifts from SA (*m*/*z* 332). The main metabolite M2 (*m*/*z* 320) resulted from ring-cleavage of SA followed by demethylation, whereas M4 (*m*/*z* 348) is oxidized by CYP in the presence of NADPH. The diol-sanguinarine metabolite M6 (*m*/*z* 366) formed by RLM might derive from a putative epoxy-sanguinarine metabolite M5 (*m*/*z* 348). M4 and M6 could be detected in rat urine as their respective glucuronides. 5,6-Dihydrosanguinarine is the prominent derivative formed from SA in cells expressing no CYP. Oxidative biotransformation of SA was investigated using eight human CYPs: only CYP1A1 and CYP1A2 displayed activity.

1. Introduction

Sanguinarine (SA) is a quaternary benzo[*c*]phenanthridine alkaloid (Fig. 1a) present in *Paperveraceae*, particularly in *Argemone mexicana* L. seed and in the rhizome of *Sanguinaria canadensis* L. SA toxicity has been evidenced during Epidemic Dropsy (ED) in India resulting from the consumption of mustard oil educorated by *Argemone* oil. Several outbreaks of dropsy have been reported in 1998 in Delhi. Recently largest outbreak of ED appeared in the country involving over 2992 victims admitted to hospital and more than 67 deaths [1]. Although SA exhibits anti-bacterial and anti-inflammatory properties, *in vitro* studies using various human cells demonstrate that SA is a toxic compound exhibiting potential antitumor activity, as reported by Karp et al. [2]. SA is shown to bind with rat tubulin to inhibit the microtubule polymerization and can readily intercalate double-stranded DNA, causing DNA single strand breaks. Due to its structural similarity with polycyclic aromatic hydrocarbons, SA might act as a potential procarcinogen. Moreover, aryl hydrocarbon receptor metabolic signalling pathways might modulate SA activity, according to Karp et al. [2]. Recently, *in vitro* metabolism studies in rat showed that cytochrome P4501A1 (CYP1A1) and P4501A2 (CYP1A2) were involved in SA metabolism. Thus, Vrba et al. [3] report that CYP1A2 could likely modulate SA toxicity. A few toxicological studies of SA have been recently conducted in animals [4]. Williams et al. [5] demonstrate that administration of SA (10 mg/kg mice) results in significant decrease of liver glutathione and CYP enzymes activities. SA is reduced [6] into 5,6-dihydrosanguinarine (DHSA), identified in rat plasma and liver by liquid chromatography–electrospray ionization-mass spectrometry (LC–ESI-MS) [7]. A pharmacokinetic study of DHSA [8] shows recently no toxicity in rat using repeated dosing of 58 mg/kg/day. Actually SA toxicity mechanism may be partially explained by the production of reactive oxygen species such as peroxide oxygen [9] generated by enzyme-catalyzed redox cycling between the reduced and oxidized forms of phenanthridine. SA cytotoxicity is probably due to a rapid apoptotic response induced by a glutathione depletion effect [10], as demonstrated also in plasma of ED patients by Babu et al. [11]. Recently, Ansari et al. [12] suggested that antioxidants such as riboflavin might provide protection to ED patients in case of acute toxicity with *Argemone*.

A combination of complementary approaches is required to identify enzyme(s) responsible for the biotransformation of xenobiotics. Once the enzymes known, prediction may be

* Corresponding author. Tel.: +33 142116009; fax: +33 142115308.
E-mail address: alain.deroussent@igr.fr (A. Deroussent).

0731-7085/$ – see front matter © 2009 Elsevier B.V. All rights reserved.
doi:10.1016/j.jpba.2009.09.014

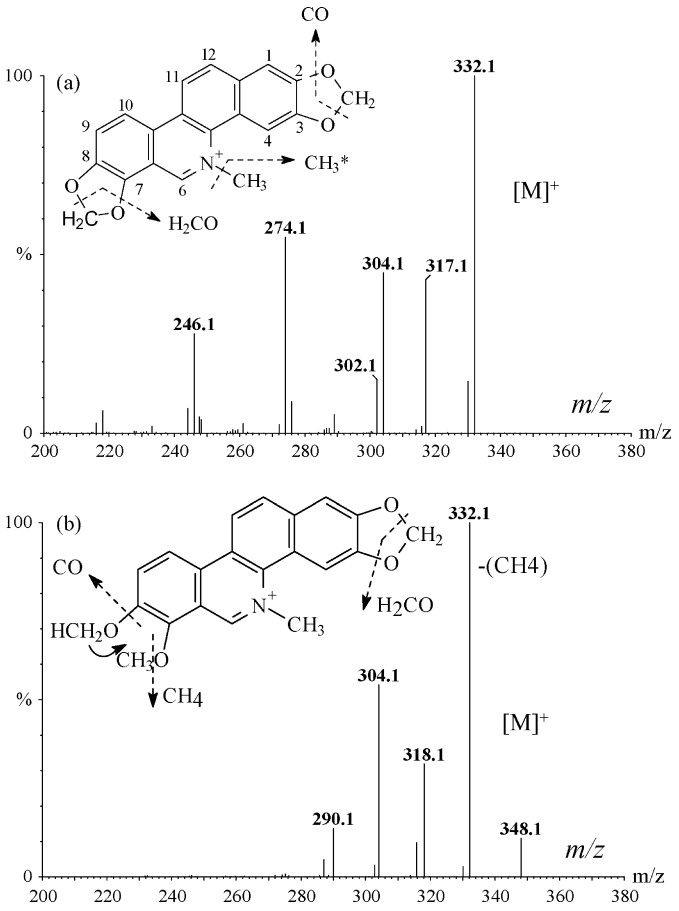

Fig. 1. Mass spectrum and proposed fragment ion pathways of (a) SA and of (b) CHEL.

made concerning drug–drug interactions potentially resulting in clinical alteration of pharmacokinetics. Very sensitive HPLC methods coupled to fluorescence detection [13,14] or electrospray ionization-mass spectrometry (ESI-MS) [7] are required for quantifying SA in culture medium or in rat plasma or urine. Thus, the biotransformation of SA and chelerythrine (CHEL, Fig. 1b) into dihydro derivatives has been successfully characterized by LC–ESI-MS [7,15].

Previous *in vitro* studies [2] indicated that CYP-dependent mono-oxygenations were involved in SA metabolism. These investigations conducted with rat or human liver microsomes suggested modulation by CYP1A. In order to understand the toxicity of SA, its metabolism is studied *in vitro* using induced RLM. Then, SA incubations were conducted with human recombinant CYP to characterize the human metabolic pathway(s) undergone by SA and to identify the CYP isoforms involved in these oxidative reactions. In the present work, LC–ESI-MS/MS was used allowing the characterization of major and minor oxidative SA metabolites produced by human CYP1A (Fig. 2) and RLM in order to do their structural elucidation in comparison with CHEL metabolites formed by RLM. *In vivo* SA metabolic experiments in rat were performed in order to provide additional information about SA detoxification pathways.

2. Experimental

2.1. Chemicals

SA (13-methyl[1,3]benzodioxolo[5,6-*c*]-1,3-dioxolo[4,5-*i*] phenanthridinium), CHEL (1,2-dimethoxy-12-methyl[1,3] benzodioxolo[5,6-*c*]phenanthridinium), glucose-6-phosphate, glucose-6-phosphate dehydrogenase, nicotinamide adenine dinucleotide phosphate (NADP), ketoconazole (KETO), triacetyloleandomycin (TAO), sulfophenazole (SF), trichloropropane oxide (TCPO), β-naphtoflavone (BNF) and β-glucuronidase were provided by Sigma–Aldrich (St Louis, MO, USA). Aroclor 1254 was obtained from Monsanto (St Louis, MO, USA). HPLC-grade

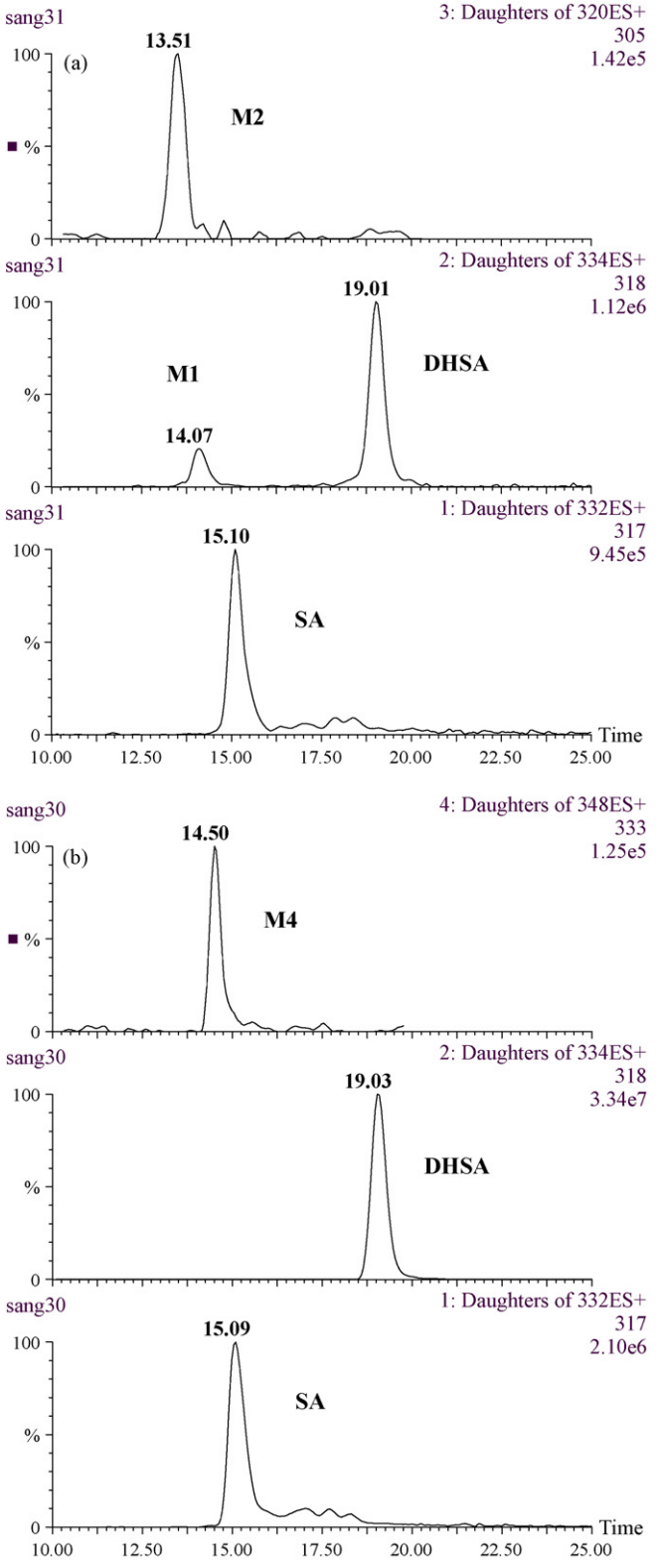

Fig. 2. LC–MS/MS chromatograms of SA incubations with (a) human CYP1A1 and (b) human CYP1A2.

acetonitrile, methanol and formic acid were purchased from Carlo Erba (Val-de-Reuil, France). Water was purified and filtered using a Milli-Q system (Millipore, St Quentin-en-Yvelines, France).

2.2. Rat urine

Three male Sprague–Dawley rats (mean body weight of 150 g) were provided by Janvier (Le Genest St Isle, France). After 12 h fasting, they were administrated *per os* with a single dose of SA (10 mg/kg body weight). Urine was collected after 12 and 48 h and analyzed before and after incubation with β-glucuronidase (1000 IU/ml) for 2 h at 37 °C.

2.3. RLM

Livers were obtained from three non-induced male Sprague–Dawley rats or from three rats treated with 500 mg/kg Aroclor 1254 once daily for 3 days or with 80 mg/kg BNF, inducer of CYP1A1/2. Microsomes were prepared according to Abernathy et al. [16] and protein concentration of 1 mg/ml was measured using the micro-BCA protein reagent assay (ref. 23224, Pierce, Rockford, IL, USA). The CYP content concentration was determined using the method described by Omura and Sato [17]. Incubations (final volume 0.5 ml) were performed with 0.5 mg RLM in 100 mM phosphate buffer (pH 7.4) containing 20% glycerol and 10 mM $MgCl_2$. After pre-warming for 10 min at 37 °C, in the presence of a NADPH-generating system consisting in 1.5 mM NADP, 2.5 mM glucose-6-phosphate and 2 IU glucose-6-phosphate dehydrogenase, the incubation was initiated by the addition of substrate (SA or CHEL) at a final concentration of 5 μg/ml (15 μM) and was stopped after 30 or 60 min by the addition of 5 ml of the extraction solvent.

2.4. Inhibition of SA metabolism in RLM

The *in vitro* inhibition of SA metabolism was carried out with RLM by inactivation with heating at 100 °C for 4 min (positive control), or after inactivating flavine monooxygenase by heating at 42 °C for 3 min, in the presence or absence of NADPH-generating system, with or without of SA. The following CYP inhibitors, CYP3A4/5-specific inhibitor KETO, CYP2C6 specific inhibitor SF, CYP3A1/2-specific inhibitors TAO and SKF-525 were used at the respective concentrations of 30, 10, 10 and 300 μM. Epoxide hydrolase was inhibited with 15 μM of TCPO.

2.5. Incubation of SA with human recombinant CYP

Ad293 cells were maintained at 37 °C under 5% CO_2, in Dulbecco's modified Eagle's medium supplemented with 4500 mg/l D-glucose, 10% fetal calf serum, 100 IU/ml penicillin and 100 μg/ml streptomycin. The preparation of stably transfected Ad293 cells expressing CYP1A1, 1A2, 2A6, 2C8, 2C9, 2C19, 2D6, 3A4, 3A5 and 3A7 was detailed previously [18]. SA (5 μM final concentration) was incubated with 5 ml of culture medium at 37 °C in 75-cm^3 flasks containing either mock-transfected Ad 293 cells or human CYP-expressing cells lines at near confluence. After 24 h, the culture medium was removed and processed as follows.

2.6. Sample preparation

Microsomes incubations, cell culture media and rat urine samples (0.5 ml) were extracted by addition of 5 ml of ice-cold acetonitrile–methanol (50:50, v/v) containing 0.2% formic acid. After 10 min shaking, samples were centrifuged at 10 000 × *g* for 20 min at 4 °C. Organic fractions were removed, evaporated to dryness under nitrogen and dissolved in 200 μl of eluent A, water–acetonitrile (80:20, v/v) with 0.1% formic acid.

2.7. HPLC/UV

Extracted rat urine samples were analyzed with the HPLC system (Waters, St Quentin en-Yvelines, France) consisted in a 600 pump controller, two 510 pumps and a 712 WISP autosampler, fitted with a C18 10 μm Symmetry column (250 mm × 4.6 mm i.d.) running at room temperature. Isocratic elution was performed with acetonitrile–water–acetic acid (75:25:0.1, v/v), at a flow rate set at 1 ml/min. The detection was carried out with a 486 UV detector set at 327-nm wavelength. The HPLC system and detectors were controlled and data processing by the Waters Millenium® chromatography manager software.

2.8. LC–ESI-MS/MS

Rat and human samples were analyzed by LC–MS using the HP1100 series HPLC system (Agilent Technologies, Waldbronn, Germany). The HPLC consisted in a binary pump, a vacuum solvent degasser and an autosampler, fitted with a C18 5 μm Nucleosil (150 mm × 1 mm i.d.) supplied by Interchim (Montluçon, France). The 10-min linear gradient was carried out from 100% of eluent A to 100% of eluent B, water–acetonitrile (95:5, v/v) with 0.1% formic acid. The flow rate was set at 50 μl/min. SA and its metabolites were detected with electrospray ionization–tandem mass spectrometry (ESI-MS/MS). The Quattro-LCZ® triple quadrupole mass spectrometer (Waters, Manchester, UK) was operated in positive mode. The capillary voltage and the cone voltage were set at 3500 and 35 V, respectively. Nitrogen nebulizer and desolvatation gas flows were set at 50 and 300 l/h, respectively. The collision energy was set at 30 eV using argon as collision gas. The quadrupole analyzer was set at unit resolution (FWHM of 0.7 Th). The LC–ESI-MS and LC–ESI-MS/MS chromatograms were obtained by scanning over *m*/*z* 200–600 range. The product ion mass spectra of SA metabolites were performed using collision-induced dissociation of the selected precursor ions with Masslynx® software (Micromass, Waters, Manchester, UK).

3. Results and discussion

3.1. Characterization of SA metabolites by LC–ESI-MS/MS

The LC–ESI-MS/MS method was used for characterization of SA derivatives. SA has a $[M]^+$ at *m*/*z* 332 (Fig. 1a), whereas for DHSA the pseudo-molecular ion $[M+H]^+$ shifts to *m*/*z* 334 (Table 1). Three SA derivatives termed M1, M2 and M3 gave $[M]^+$ respectively at *m*/*z* 334, 320 and 336.

The first polar metabolite M1 has a $[M]^+$ at *m*/*z* 334 (Table 1), that is the same ion as that of DHSA, but they have different t_R (14.0 min versus 19.0 min). Moreover, they show different fragment ions *m*/*z* 319 (loss of methyl) and *m*/*z* 318 (loss of methane), as shown in Table 1. On the other hand, the product ion spectra of metabolites M1 and C3 (Table 2) are identical. Thus, M1 could be an *O*-demethylated CHEL derivative. The methoxy group of metabolite M1 could be located at position C-7 or C-8, as with CHEL structure (Fig. 1b). Similar biotransformation of SA and CHEL were observed: metabolites M1 and C3 were formed by ring-cleavage of SA and CHEL, respectively.

The second polar metabolite M2 has its $[M]^+$ at *m*/*z* 320, with a t_R of 13.5 min. The fragmentation of M2 yielded ions at *m*/*z* 305 (methyl loss), 292 (28 Da loss), 290 (15 Da loss from *m*/*z* 305), 262 (a further loss of 30 Da from *m*/*z* 292). The other loss of 28 Da (loss of CO from *m*/*z* 292) could indicate that the hydroxylation of one methyl group occurred at C-7 or C-8 (Fig. 3). Thus, metabolite M2

Table 1
Molecular mass, product ions and LC–MS retention times of SA and its derivatives. (1) These metabolites were only detected by LC–MS in SA incubations with Aroclor- or BNF-induced RLM.

Metabolites of SA with human CYP or RLM	Molecular ion (*m*/*z*)	Product ions (*m*/*z*)	Neutral loss	t_R (min)
SA (M = 332)	332.1	317, 304, 274, 246	CH_3*, CO, H_2CO	15.1
DHSA (M = 333)	334.1	318, 304, 276	CH_4, CO, H_2CO	19.0
Ring-cleavage of SA (M1 = 334).	334.1	319, 304, 291, 276, 263	CH_3*, CO, H_2CO	14.0
O-Demethylation of metabolite M1 (M2 = 320)	320.1	305, 290, 292, 262	CH_3*, CO, H_2CO	13.5
Ring-cleavage of metabolite M1 (M3 = 336)	336.1	321, 306, 278	CH_3*, CO, H_2CO	13.8
Hydroxy-sanguinarine (M4 = 348)	348.1	333, 320, 290, 262	CH_3*, CO, H_2CO	14.7
Epoxy-sanguinarine (1) (M5 = 348)	348.1	333, 320, 305, 262	CH_3*, CO, H_2CO	18.3
Diol-sanguinarine (1) (M6 = 366)	366.1	349, 334, 317, 285	H_2O, CO	10.0

Table 2
Molecular mass, product ions and LC–MS retention times of CHEL and its metabolites (C1–C3) produced with RLM.

Metabolites of CHEL with RLM	Molecular ion (*m*/*z*)	Product ions (*m*/*z*)	Neutral loss	t_R (min)
CHEL (M = 348)	348.1	332, 318, 304, 290	CH_4, H_2CO, CO	14.5
5,6-Dihydrochelerythrine (C = 349)	350.1	334, 320, 304, 276	CH_4, H_2CO, CO	19.6
Ring-cleavage of CHEL (C1 = 350)	350.1	334, 335, 320, 306, 290	CH_4, CO, H_2CO	13.5
O-Demethylation of metabolite C1 (C2 = 336)	336.1	320, 306, 292, 278	CH_4, CO, H_2CO	13.8
O-Demethylation of CHEL (C3 = 334).	334.1	319, 304, 291, 276, 263	CH_3*, CO, H_2CO	14.0

could be formed by ring-cleavage of SA followed by demethylation.

Metabolite M3 has a t_R of 13.8 min, close to M2. It has a $[M]^+$ at *m*/*z* 336 and shows a mass shift of +16 or +2 Da compared to M2 or M1, respectively. Metabolite M3 could result from a hydroxylation of M2 or from a second ring-cleavage of M1. As SA metabolic pathways, catalyzed by CYP1A1, are ring-cleavage or demethylation producing M1, M2 and M3, the hydroxylation of metabolite M2 catalyzed by CYP1A2 is unlikely. Thus, as the fragmentation data of metabolites M3 and M1 show a difference of 2 Da, metabolite M3 could be formed with cleavage of the second methylenedioxy group. Moreover, a methyl loss (*m*/*z* 321) observed for metabolite M1 suggests that the proposed structure of M3 has likely two non-adjacent hydroxy and methoxy groups, located at C-2 or C-3 and at C-7 or C-8. By comparison, a methane loss was observed with the two adjacent methoxy groups of CHEL and C2 (Table 2).

Metabolite M4 has a $[M]^+$ at *m*/*z* 348 (100%), with t_R of 14.7 min, close to that of SA (t_R 15.1 min). The fragmentation of M4 yielded ions at *m*/*z* 333 (methyl loss), *m*/*z* 320 (28 Da loss), *m*/*z* 290 (loss of 30 Da from *m*/*z* 320) and *m*/*z* 262 (a further loss of 28 Da from *m*/*z* 290). As M4 shows a mass shift of +16 Da, it could be a hydroxylated SA derivative. The hydroxy group could be probably located on a SA phenyl ring and its position might be assigned by nuclear magnetic resonance (NMR) spectroscopy, as reported for 10-hydroxy-sanguinarine isolated from cell culture [19].

Metabolite M5 has a $[M]^+$ molecular ion at *m*/*z* 348 (30%). Its mass spectrum (Fig. 4) shows an intense product ion *m*/*z* 333 (methyl loss) and a different fragment ion *m*/*z* 305, not present in the mass spectrum of M4. Moreover, M5 has a longer t_R of 18.3 min compared to that of M4 and close to that of DHSA. Based on these observations, as the quaternary ammonium is unchanged, M5 might be rather an epoxy- than a hydroxy-sanguinarine derivative. The proposed structure of M5 could be further confirmed by ESI-MS analysis of SA incubation in RLM using an epoxide hydrolase inhibitor.

Furthermore, when longer incubation in RLM was performed, a secondary derivative termed M6 (*m*/*z* 366) was detected with a mass difference of +18 Da compared to M5 (Table 1). Thus, its proposed structure might be in agreement with a diol-sanguinarine produced from the putative epoxy-sanguinarine metabolite (M5).

A general feature in these electrospray MS/MS mass spectra was the formation of fragments corresponding to either a 15 or a 16 Da loss from the quaternary ammonium ions $[M^+]$. For SA and its derivatives, the intense fragment ion $[M\text{-}15]^+$ probably corresponds to the loss of methyl radical (Fig. 1a). For CHEL (Fig. 1b), the intense fragment ion $[M\text{-}16]^+$ corresponds likely to the loss of methane resulting from the presence of the two methoxy groups located at adjacent C-7 and C-8 positions (Table 2) as demonstrated previously for ethoxidine [20]. The dissociation mechanism for CHEL was similar as those observed with ethoxidine, leading by rearrangement to a methylenedioxy ring and to a loss of CO.

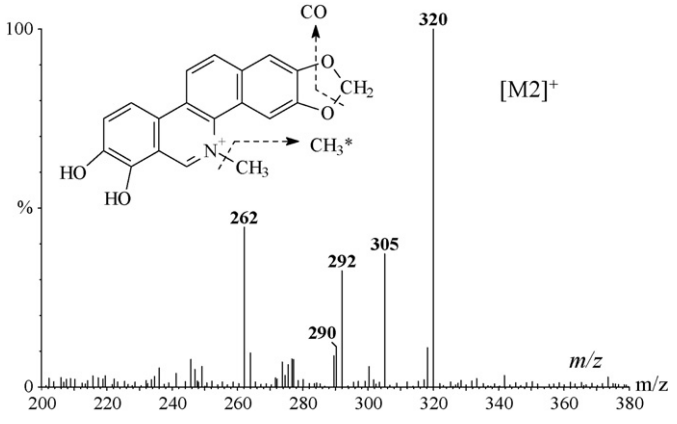

Fig. 3. ESI product ion spectrum and proposed structure of metabolite M2.

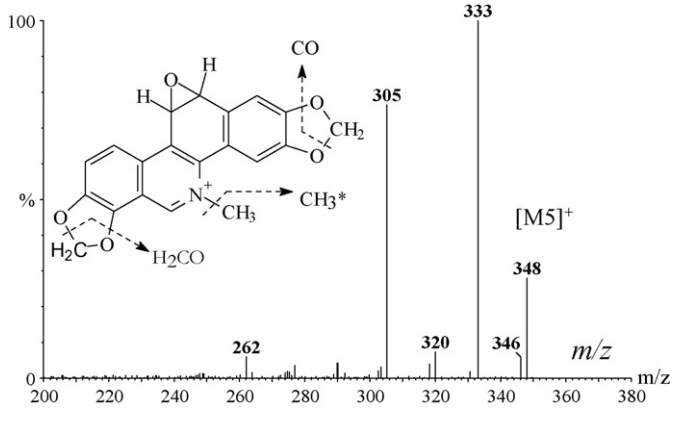

Fig. 4. ESI product ion spectrum and proposed epoxy-sanguinarine structure of metabolite M5.

3.2. Biotransformation of SA by RLM

When SA was incubated with RLM in the presence of NAPDH, no oxidative SA derivative was observed, except DHSA. Two oxidative SA metabolites (M4 and M5) were produced with non-induced and BNF-treated RLM. The presence of four SA metabolites (M1-M4) in the SA incubation with Aroclor-induced RLM and with NADPH was demonstrated by LC–ESI-MS/MS (Table 1). On the other hand, this strongly suggested that CYP1A1 and/or CYP1A2 present in BNF- or in Aroclor-induced RLM could be responsible for SA biotransformation. After the incubation time of 30 min, four peaks were detected in variable amounts. M1 and M3, eluting with respective t_R of 14.0 and 13.8 min, were two minor compounds accounting for respectively 1% and 2% of the substrate concentration, whereas M2 and M4 were two major metabolites produced by Aroclor-induced RLM (respective t_R of 13.5 and 14.5 min) corresponding to 62% and 5% of the substrate concentration. In non-induced RLM with NADPH, relative yields for M1, M4 and M5 were 3%, 3% and 2%, respectively, whereas in BNF-induced RLM, yields for M4 and M5 increased up to 7% and 16%.

3.3. Biotransformation of SA by human CYP

No oxidative derivative was observed when SA was incubated with control cells (not shown). Derivatives formed during SA incubation with cells expressing human recombinant CYP have the same t_R as those generated by RLM (Table 1). Among CYP1A1, 1A2, 1A6, 2C8, 2C9, 2D6, 3A4, 3A5 and 3A7, only CYP1A1 was capable generating up to three metabolites (Fig. 2a), whereas CYP1A2 produced only M4 (Fig. 2b). The production of M1, M2, M3 and M4 accounted for respectively 9%, 79%, 3% and 3% of the initial substrate concentration in control cells.

3.4. Inhibition of SA metabolism in RLM

Relative yield of SA derivatives was 45%, 2%, 1% and 1% for M2, M4, M5 and M6, respectively, when SA was incubated for 30 min with Aroclor-treated RLM.

TCPO is a known inhibitor of microsomal epoxide hydrolase: the production of diol-sanguinarine metabolite (M6) was completely suppressed in incubations performed in the presence of TCPO (Fig. 5b) compared to incubations without TCPO (Fig. 5a). Additionally, the formation of the two oxidative derivatives M2 and M5 was decreased by 50%, whereas the remaining content of SA and the production of M4 were increased by 50% (Fig. 5b). It suggested that epoxide hydrolase could play an active role in the formation of the oxidative SA derivatives. In the presence of non-specific inhibitors (CO and SKF525A) or after denaturation by heating at 42 or 100 °C, the production of oxidative derivatives was severely impaired with a suppression of M2 and a high decrease of M4. When incubations were performed with more specific inhibitors, the production of derivatives remained unchanged with CYP 2C9 inhibitor SF and as well with CYP 3A inhibitors KETO and TAO.

3.5. In vivo SA metabolism in rat

Additional *in vivo* experiments were performed in rat to confirm the biotransformation of SA by RLM. Two major peaks were detected by HPLC/UV analysis (not shown) in acidic extracts of rat 12 h urine and identified by ESI-MS as SA (t_R 6.9 min; m/z 332) and DHSA (t_R 8.0 min; m/z 334). Two peaks (1) and (2) detected by UV had shorter t_R of 3.3 and 4.4 min and molecular ions at m/z 541 and m/z 525, respectively. The incubation of urine samples with β-glucuronidase resulted in the complete loss of these two peaks and the occurrence of two peaks at t_R = 6.0 min (3) and t_R = 6.2 min (4). The mass spectrum of peak 3 showed a $[M]^+$ at m/z 366 compatible with M6 ascertained as diol-sanguinarine (Table 1). The mass spectrum of peak 4 showed a $[M]^+$ at m/z 348 and a fragment of m/z 333, compatible with M4 ascertained as hydroxy-sanguinarine (Table 1).

The polar compound present in peak 2 displayed a $[M]^+$ of m/z 525 and a specific fragment ion (m/z 349) with a neutral loss of 176 Da, corresponding to a glucurosonyl moiety. Thus, it could correspond to a glucuronide of the hydroxylated SA derivative, M4. The polar derivative present in peak 1 displayed a $[M]^+$ of m/z 541 and a specific fragment ion (m/z 366) identical to that of M6 with a neutral loss of 176 Da and could probably correspond to M6 glucuronide. A putative structure of metabolite M6 could be proposed as 9,10- or 11,12-diol-sanguinarine formed after the hydroxylation of the primary metabolite M5, epoxy-sanguinarine.

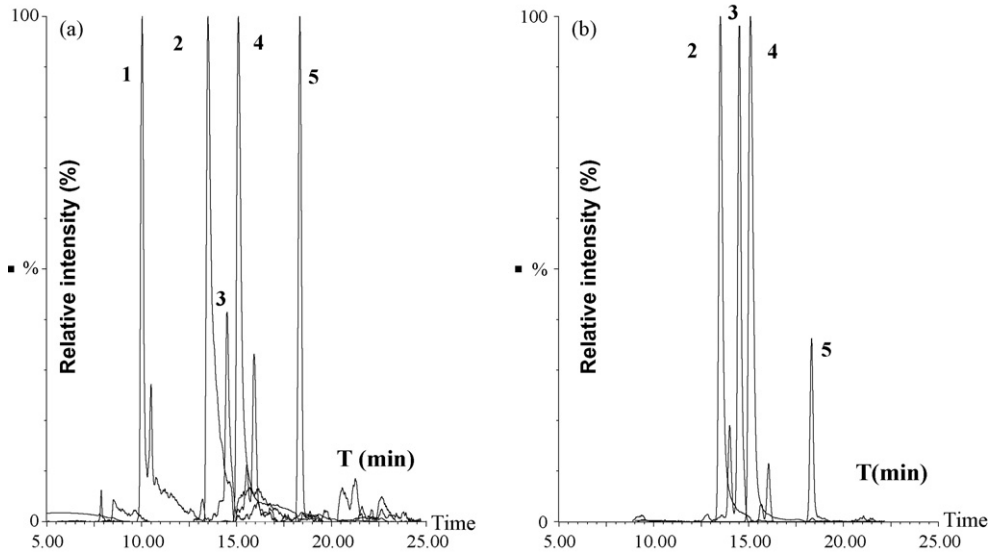

Fig. 5. LC–MS chromatograms of SA incubations in Aroclor-induced RLM (a) without or (b) with TCPO. Peak characterization: (1) diol-sanguinarine (M6); (2) *O*-demethylated metabolite (M2); (3) hydroxy-sanguinarine (M4); (4) SA; (5) epoxy-sanguinarine (M5).

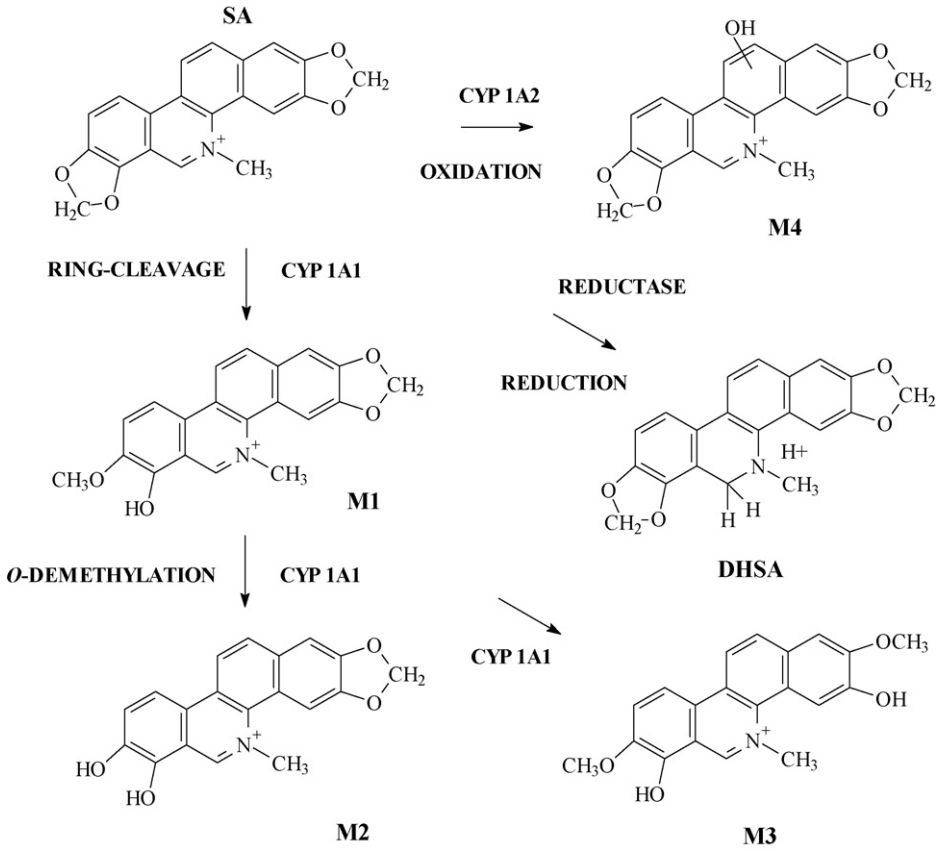

Fig. 6. Proposed metabolic pathways of SA by human CYP1A1 and CYP1A2 (structures of metabolites are tentative ones).

3.6. Metabolic pathways of SA

SA metabolism was studied in human CYP and in RLM in order to tentatively characterize oxidative metabolites of SA. Oxidative biotransformation of SA was investigated using eight human CYPs: only CYP1A1 and CYP1A2 displayed activity. Thus, metabolic pathways of SA by CYP1A1 and by CYP1A2 (Fig. 6) could be proposed. First, SA was shown to be transformed into the non-toxic DHSA [7] under the action of CYP reductase, present either in rat liver [9] or in human CYP cells lines [21]. SA could be oxidized into hydroxylated metabolites by CYP1A2 or *O*-demethylated by CYP1A1.

On one hand, the oxidative SA metabolic pathway produced by CYP1A2 is hydroxylation like for caffeine [22]. On the other hand, the two-step biotransformation of SA into a derivative M2 is overall an *O*-demethylenation, already observed for methylenedioxymethamphetamine by Fonsart et al. [23].

The CYP1A1 oxidative route, associated with epoxide hydrolase, should be an important detoxification route for electrophilic compounds such as quaternary benzo[*c*]phenanthridine alkaloids [24] and may explain the formation of a diol-sanguinarine metabolite (M6) generated from the proposed epoxy-sanguinarine (M5). CYP1A1 oxidizes small molecules featuring a planar structure and capable of participating in aromatic π–π interactions and hydrogen-bonding interactions with amino acids of the protein like benzo[*a*]pyrene, dimethylbenzanthracene and aflatoxin, to primarily epoxides that are further hydrated to the corresponding dihydrodiols [25–27]. From this point of view, SA fits with the theoretical structure required to be a good substrate of CYP1A1.

4. Conclusion

Four SA metabolites were formed by human CYP in transfected cells, whereas six were found in RLM incubations. Metabolite M2 resulted from ring-cleavage of SA followed by demethylation, whereas M4 is oxidized by CYP in the presence of NADPH. Metabolites M4 and M6 formed by RLM are detected in rat urine as their respective glucuronides. The proposed structure of these metabolites could be further confirmed by NMR analysis of purified rat samples. DHSA is the main derivative formed from SA in cells expressing no CYP. Oxidative biotransformation of SA involved only CYP1A1 and CYP1A2 among the eight investigated human CYPs.

References

[1] M. Das, S.K. Khanna, Clinicoepidemiological, toxicological, and safety evaluation studies on argemone oil, Crit. Rev. Toxicol. 27 (1997) 273–297.
[2] J.M. Karp, K.A. Rodrigo, P. Pei, M.D. Pavlick, J.D. Andersen, D.J. Mc Tigue, H.W. Fields, S.R. Mallery, Sanguinarine activates polycyclic aromatic hydrocarbon associated metabolic pathways in human oral keratinocytes and tissues, Toxicol. Lett. 158 (2005) 50–60.
[3] J. Vrba, P. Kosina, J. Ulrichová, M. Modriansky, Involvement of cytochrome P450 1A in sanguinarine detoxication, Toxicol. Lett. 151 (2004) 375–387.
[4] P. Kosina, D. Walterová, J. Ulrichová, V. Lichnovský, M. Stiborová, H. Rýdlová, J. Vicar, V. Krecman, M.J. Brabec, V. Simánek, Sanguinarine and chelerythrine: assessment of safety on pigs in ninety days feeding experiment, Food Chem. Toxicol. 42 (2004) 85–91.
[5] M.K. Williams, S. Dalvi, R.R. Dalvi, Influence of 3-methylcholanthrene pretreatment on sanguinarine toxicity in mice, Vet. Hum. Toxicol. 42 (2000) 196–198.
[6] D. Weiss, A. Baumert, M. Vogel, W. Roos, Sanguinarine reductase, a key enzyme of benzophenanthridine detoxification, Plant Cell Environ. 29 (2006) 291–302.
[7] J. Psotová, B. Klejdus, R. Vecera, P. Kosina, V. Kubán, J. Vicar, V. Simánek, J. Ulrichová, A liquid chromatographic-mass spectrometric evidence of dihydrosanguinarine as a first metabolite of sanguinarine transformation in rat, J. Chromatogr. B: Anal. Technol. Biomed. Life Sci. 830 (2006) 165–172.
[8] E. Vrublova, J. Vostalova, R. Vecera, B. Klejdus, D. Stejskal, P. Kosina, A. Zdarilova, A. Svobodova, V. Lichnovsky, P. Anzenbacher, Z. Dvorak, J. Vicar, V. Simanek, J. Ulrichova, The toxicity and pharmacokinetics of dihydrosanguinarine in rat: a pilot study, Food Chem. Toxicol. 46 (2008) 2546–2553.
[9] S.S. Matkar, L.A. Wrischnik, U. Hellmann-Blumberg, Production of hydrogen peroxide and redox cycling can explain how sanguinarine and chelerythrine

induce rapid apoptosis, Arch. Biochem. Biophys. 477 (2008) 43–52.
[10] E. Dubiton, J.C. Madelmont, J. Legault, C. Barthomeuf, Sanguinarine-induced apoptosis is associated with an early and severe cellular glutathione depletion, Cancer Chemother. Pharmacol. 51 (2003) 474–482.
[11] Ch.K. Babu, K.M. Ansari, S. Mehrotra, R. Khanna, S.K. Khanna, M. Das, Safety evaluation studies on argemone oil through dietary exposure for 90 days in rats, Food Chem. Toxicol. 46 (2008) 2409–2414.
[12] K.M. Ansari, A. Dhawan, S.K. Khanna, M. Das, Protective effect of bioantioxidants on argemone oil/sanguinarine alkaloid induced genotoxicity in mice, Cancer Lett. 244 (2006) 109–118.
[13] M. Klvana, J. Chen, F. Lépine, R. Legros, M. Jolicoeur, Analysis of secondary metabolites from eschscholtzia californica by high-performance liquid chromatography, Phytochem. Anal. 17 (2006) 236–242.
[14] H. Hoellinger, M. Ré, A. Deroussent, R.P. Singh, T. Cresteil, Quantitative liquid chromatographic determination of sanguinarine in cell culture medium and in rat urine and plasma, J. Chromatogr. B: Anal. Technol. Biomed. Life Sci. 799 (2004) 195–200.
[15] B. Klejdus, L. Lojková, P. Kosina, J. Ulrichová, V. Simánek, V. Kubán, Liquid chromatographic/electrospray mass spectrometric determination (LC/ESI-MS) of chelerythrine and dihydrochelerythrine in near-critical CO(2) extracts from real and spiked plasma samples, Talanta 72 (2007) 1348–1356.
[16] C.O. Abernathy, E. Hodgson, F.E. Guthrie, Structure–activity relationships on the induction of hepatic microsomal enzymes in the mouse by 1,1,1-trichloro-2,2-bis(p-chlorophenyl) ethane(DDT) analogs, Biochem. Pharmacol. 21 (1971) 2385–2393.
[17] T. Omura, R. Sato, The carbon monoxide-binding pigment of liver microsomes. II. Solubilization, purification, and properties, J. Biol. Chem. 239 (1964) 2379–2385.
[18] M. Sonnier, T. Cresteil, Delayed ontogenesis of CYP1A2 in the human liver, Eur. J. Biochem. 251 (1998) 893–898.
[19] T. Tanahashi, M.H. Zenh, New hydroxylated benzo[c]phenanthridine alkaloids from Eschscholtzia californica cell suspension cultures, J. Nat. Prod. 53 (1990) 579–586.
[20] A. Deroussent, M. Ré, H. Hoellinger, E. Vanquelef, O. Duval, M. Sonnier, T. Cresteil, In vitro metabolism of ethoxidine by human CYP1A1 and rat microsomes: identification of metabolites by high-performance liquid chromatography combined with electrospray tandem mass spectrometry and accurate mass measurements by time-of-flight mass spectrometry, Rapid Commun. Mass Spectrom. 18 (2004) 1–9.
[21] J. Vrba, P. Dolezel, J. Vicar, J. Ulrichová, Cytotoxic activity of sanguinarine and dihydrosanguinarine in human promyelocytic leukemia HL-60 cells, Toxicol. In Vitro 23 (2009) 580–588.
[22] M. Kot, W.A. Daniel, The relative contribution of human cytochrome P450 isoforms to the four caffeine oxidation pathways: an in vitro comparative study with cDNA-expressed P450s including CYP2C isoforms, Biochem. Pharmacol. 75 (2008) 1538–1549.
[23] J. Fonsart, M.C. Menet, X. Declèves, H. Galons, D. Crété, M. Debray, J.M. Scherrmann, F. Noble, Sprague–Dawley rats display metabolism-mediated sex differences in the acute toxicity of 3,4-methylenedioxymethamphetamine (MDMA, ecstasy), Toxicol. Appl. Pharmacol. 230 (2008) 117–125.
[24] L. Soleo, The detoxification pathways of electrophilic intermediate compounds, Med. Lav. 85 (1994) 22–36.
[25] M. Shou, K.R. Korzekwa, C.L. Crespi, F.J. Gonzalez, H.V. Gelboin, The role of 12 cDNA-expressed human, rodent, and rabbit cytochromes P450 in the metabolism of benzo[a]pyrene and benzo[a]pyrene trans-7,8-dihydrodiol, Mol. Carcinog. 10 (1994) 159–168.
[26] M. Shou, K.R. Korzekwa, K.W. Krausz, J.T. Buters, J. Grogan, I. Goldfarb, J.P.H. Ardwick, F.J. Gonzalez, H.V. Gelboin, Specificity of cDNA-expressed human and rodent cytochrome P450s in the oxidative metabolism of the potent carcinogen 7,12-dimethylbenz[a]anthracene, Mol. Carcinog. 17 (1996) 241–249.
[27] C.L. Crespi, B.W. Penman, D.T. Steimel, T. Smith, C.S. Yang, T.R. Sutter, Development of a human lymphoblastoid cell line constitutively expressing human CYP1B1 cDNA: substrate specificity with model substrates and promutagens, Mutagenesis 12 (1997) 83–89.